JOURNAL OF MATERIALS SCIENCE 23 (1988) 4085–4090

Effect of time and temperature on nonlinear constitutive equation in polypropylene

MASAYOSHI KITAGAWA, TOMOHIKO MATSUTANI
Department of Mechanical Engineering, Faculty of Technology, Kanazawa University, Kanazawa, Japan

In order to investigate viscoelastic-plastic properties and discuss a constitutive equation at finite strains in polymer solids, uniaxial compression tests were executed at different temperatures using polypropylen (PP) rods under conditions of constant strain rate, abrupt change of strain rate, stress relaxation, creep loadings and their combination. Several viscoelastic–plastic properties which must be taken into account in the constitutive equation of PP are pointed out, and the experimental data are compared with the numerical results based on the concept of an over stress model. It is found that the model describes the stress-strain behaviours of PP well in the case where the current strain is not below the previous one.

1. Introduction

The linear theory of viscoplasticity is well formulated and has been successfully applied. However, most real polymer solids are known to show non-linear viscoelastic-plastic behaviour even in small strain ranges. Although much effort has been made to introduce a non-linearlity in the linear theory and several non-linear constitutive models have been proposed, the non-linear behaviour in the plastic regions are less well understood because of many complexities peculiar to polymer materials. Therefore, in order to construct a suitable constitutive model in polymer solids, systematic experiments should be planned to demonstrate the effect of time, temperature, pressure and strain histories on the stress–strain relationship in the plastic region.

Roughly speaking, there may be two methods to construct a constitutive equation in a non-linear space of stress and strain. One is based on the plastic potential theory. This approach assumes a yield function such as Mises criterion, and is successfully applied to the behaviour of metals. In polymer solids, the phenomenon of yield is usually a gradual transition from a linear to a non-linear response. Hence it is difficult to distinguish an inelastic strain from a total strain. This vagueness may make it difficult to investigate a non-linear constitutive law from the viewpoint of the plastic potential theory.

The other method, therefore, is not based on the assumption of yield function. The endocronic theory proposed by Valanis [1, 2] and the over-stress theories proposed by Malvern [3] and Krempl [4, 5] belong to this concept. These theories are shown to describe the uniaxial stress–strain curves well not only under constant strain rate loading, but also under cyclic loading in metals.

The purpose of this paper is to point out some experimental facts up to the relatively large strain ranges, which are required for the construction of the non-linear constitutive equation in polymer solids. Then, uniaxial compression tests were performed by use of polypropylene (PP) rods at low strain rates in different temperatures, and the experimental data obtained are discussed based on one of the over-stress theories.

2. Experimental Procedure

The material used was commercial polypropylene extruded rods. After they were annealed for 2 h at 70° C, cylindrical specimens of 12 mm diameter and 18 mm height were machined from them, and then were again annealed for 2 h at 70° C. Observation using a polarized light microscope showed that the shape and diameter of spherulites are not anisotropic.

All specimens were compressed at temperatures 15, 25 and 40° C in a home-made servo-controlled machine. During the test, the height and the diameter of the specimen were recorded on a microcomputer. The true stress averaged over the cross-section of the specimen and the logarithmic strain were used for the data arrangement. To prevent the barrel type deformation of the specimen, thin polytetrafluoroethylene sheets were used as a lubricant. When the compressive strain exceeds about 0.15, the specimen does not deform uniformly along its longitudinal direction and a slight barrelling begins to occur. However, the degree of barrelling is not very large and is neglected. The compressive tests were carried out under several strain paths such as constant nominal strain rate, stress relaxation, creep and their combinations. Since the temperature rise of the specimen observed during the test was within 3° C at most in this present strain rate ranges, its effect is not considered below.

When the polymer is subjected to tension, numerous crazes initiate and grow perpendicularly to the stress direction before shear yielding occurs. Since these flaws cause inelastic deformation as described elsewhere [6], they may not obey the essential constitutive

0022–2461/88 $03.00 + .12

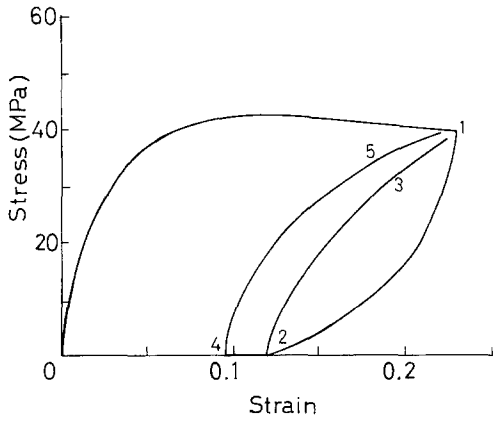

Figure 1 Uniaxial compressive stress–strain curve at a strain rate of 0.0009 sec^{-1} in PP. The path 1–2–3 denotes the case where the specimen was reloaded soon after the applied load became zero due to strain reversal. The path 1–2–4–5 shows the case where the specimen was reloaded after it was kept stress-free for 30 min.

laws. In this paper, therefore, compression tests which were free from the initiation of crazes were used.

3. Test results

3.1. General features at a constant strain rate test

After the specimen was compressed up to a predetermined strain of 0.22 and immediately unloaded at a constant strain rate ($\pm 0.0009\,sec^{-1}$), reloading was done at the same strain rate. Fig. 1 shows the stress–strain curves observed from these tests. The curve 1–2–3 denotes that obtained when reloading was carried out soon after the applied load vanished. The 1–2–4–5 curve denotes the stress–strain relation measured when the specimen was reloaded after it was left in a stress-free state for 30 min. The 2–4 part means that the strain recovery gradually occurs with an increase in the elapse time.

Fig. 2 shows the effect of the unloading path on the recovery of the applied strain. After the applied stress was removed along path a (unloading at a constant strain rate) or b (unloading at a constant strain rate after 24 h stress relaxation), the strain recovery was measured against time.

It may be shown from these data of PP that (1) a steep stress drop is not observed at yielding and the transition from the linear to the non-linear behaviours is gradual, (2) a slight work softening occurs in the regions of high strain, (3) a reversed loading curve (1–2 in Fig. 1) and reloading ones (2–3 and 4–5) are different from the initial curve 0–1, (4) residual strain after stress removal is dependent on the unloading path, (5) permanent strain is considerably small compared with the applied strain (the ratio of permanent strain to applied one is only about 1/3–1/2 in the case of the applied strain of 0.22) and so on.

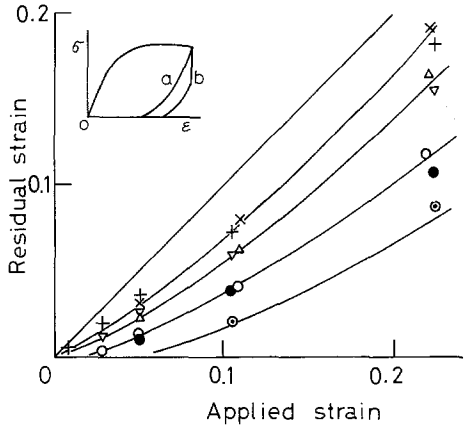

Figure 2 Effect of unloading path on residual strain. The periods during which specimens were kept stress-free after the path b are ×, +; 1 min, △, ▽; 10 min and ○, ●; 1 month. The mark ◉ shows permanent residual strains obtained after the path a.

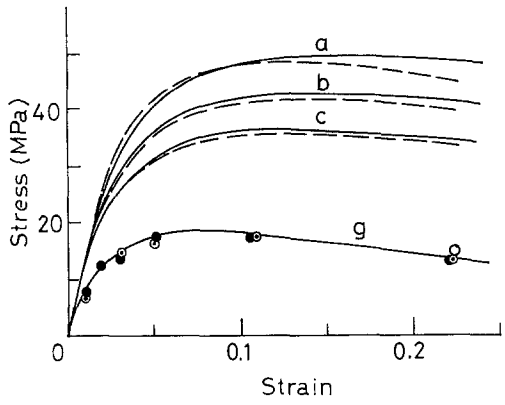

Figure 3 Experimental (– – –) and calculated (——) compressive stress–strain curves in 25° C at different strain rates of a; $9 \times 10^{-3}\,sec^{-1}$, b; $9 \times 10^{-4}\,sec^{-1}$ and c; $9 \times 10^{-5}\,sec^{-1}$. The solid curve g computed from Equation 9 is the equiribrium stress–strain curve. The circles show the experimental stress-values which were reached after the lapse of 24 h in the relaxation tests at various strains. The strain rates preceding the relaxation test are ◉; $9 \times 10^{-3}\,sec^{-1}$, ●; $9 \times 10^{-4}\,sec^{-1}$ and ○; $9 \times 10^{-5}\,sec^{-1}$.

These observations may point out that it is difficult to determine in a precise manner when yielding occurs and therefore, what stress condition governs yielding because of the vagueness of the definition of yielding and furthermore, to separate the visco-plastic strain from the total strain due to the intense time-dependent nature of residual strain. These may be very different from the stress–strain responses of metals.

In the case where the current strain is below the previous strain, the stress–strain response may become more complex than the case where the applied strain increases monotonously. In the present paper, the stress–strain relations including the path of strain reversal are not treated.

3.2. Strain rate sensitivity

The dotted lines in Fig. 3 denote the results of compression tests at three different nominal strain rates ranging from 10^{-4} to $10^{-2}\,sec^{-1}$ in 25° C. The solid lines are described later. It is found that the initial slope of the stress–strain curves is not so dependent on the strain rate and the stress–strain curves at different strain rates are nearly parallel to each other and are sensitive to the rate in the high strain ranges. The trends of the experimental curves obtained at 15 and 40° C are similar to those in the figure.

The circles in the figure denote the stress values which were reached after the stress relaxation tests were performed up to 24 h where the rates of stress decrease were very small and their relaxation limits would be reached. They seem to fall on the same

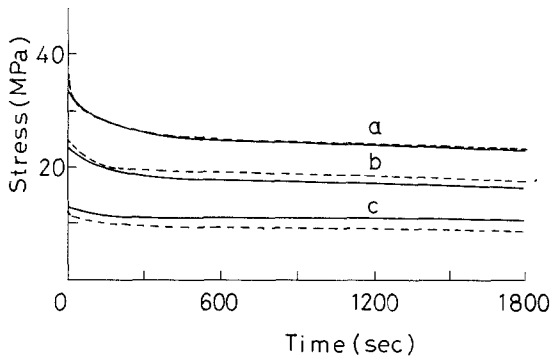

Figure 4 Comparison between experimental (– – –) and calculated (——) stress relaxation curves at 25° C. The strain rates prior to the relaxation is 9×10^{-4} sec^{-1} and the strains are a; 0.05, b; 0.02 and c; 0.01.

curve independent of the strain rate preceding the relaxation. The solid curve marked g which passes through the circles is called an equiribrium stress–strain curve which may correspond to the one measured at a very slow strain rate. The equiribrium curve also seems to have a weak strain softening.

3.3. Stress relaxation and creep

Examples of the relaxation results are denoted in Fig. 4 where the solid curves are numerically calculated. Specimens were compressed at a nominal strain rate of 0.0009 sec^{-1} to predetermined strains and then the strains were held constant. It may be found that the stress drops steeply at the beginning of the test, gradually decreases with an increase in elapsing time and seems to approach a relaxation limit which is peculiar to an applied strain and is independent of the strain rate preceding to the relaxation test. In this paper, the existence of the relaxation limit is assumed.

Fig. 5 shows the values of stress drop measured after an elapse of 1 h from the start of the relaxation tests for given applied strains. The relaxation data are plotted for the different nominal strain rates prior to the relaxation. It is seen in the tests started from the points in the relatively high strain ranges that the amount of stress relaxation for a given time interval is nearly independent of the test strain and depends on the strain rate preceding the relaxation test. Similar

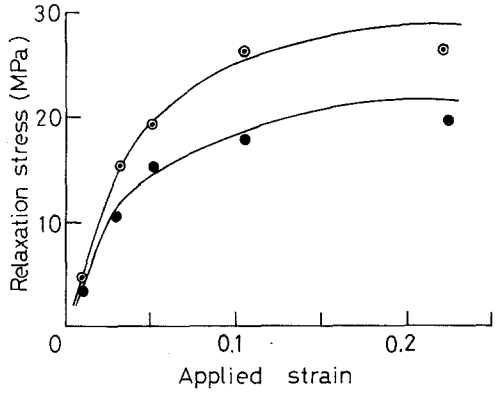

Figure 5 Comparison between experimental (●, ◉) and computed (——) values of stress drop for an interval of 1 hour in the relaxation test at 25° C. the strain rates prior to the relaxation are ●; 9×10^{-4} sec^{-1} and ◉; 9×10^{-3} sec^{-1}.

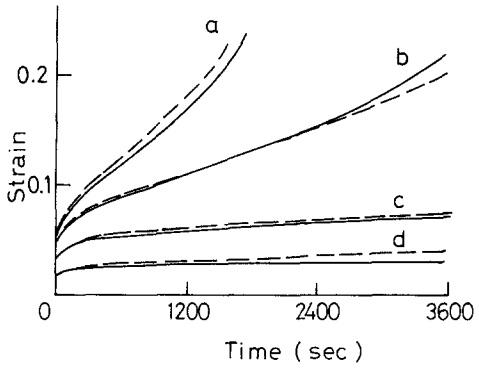

Figure 6 Experimental (– – –) and computed (——) compressive creep curves at various applied stresses (a; 31 MPa, b; 36 MPa, c; 28 MPa and d; 21 MPa) at 25° C.

trends are observed for the other relaxation periods. The solid curves are calculated.

Compressive creep behaviours are drawn in Fig. 6 where the solid curves are theoretical. After the specimen was compressed to a predetermined stress at a constant nominal-strain rate of 0.009 sec^{-1}, the net stress averaged over the specimen cross section was controlled to be kept constant by the computer signal. In the relatively high stress ranges, there exist three stages, i.e., Stage I (primary creep) where a steep increasing time and Stage III (tertiary creep) where the specimen deforms with increasing rapidity to lead to a final fracture. However, at low stresses, only two stages I and II are recognized. This feature of creep behaviour during a short period at both low and high stresses may be important for constructing a constitutive model.

3.4. Stress–strain response with complex strain histories

In this section, the effect of several complex strain histories on the stress–strain curve is discussed. Fig. 7 depicts the curve obtained from the repetition of constant nominal-strain rate (0.0009 sec^{-1}) and 60 sec stress relaxation tests. The solid line is theoretical as described later. The amount of stress drop during relaxation is nearly constant independent of the strain in the high strain ranges. This trend is nearly the same as shown in Fig. 5. At constant rate compression after the 60 sec relaxation, the stress–strain curve has an elastic response near the change point and gradually

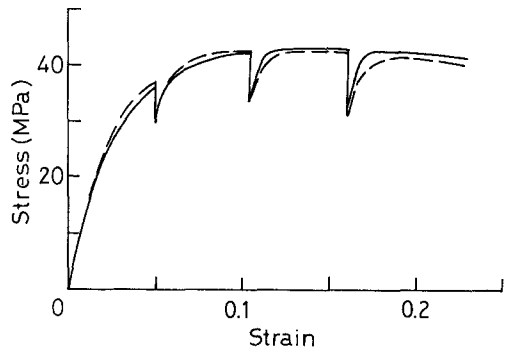

Figure 7 Experimental (– – –) and computed (——) stress–strain curve at the repetition of constant nominal strain rate compression and 60 sec stress relaxation at 25° C.

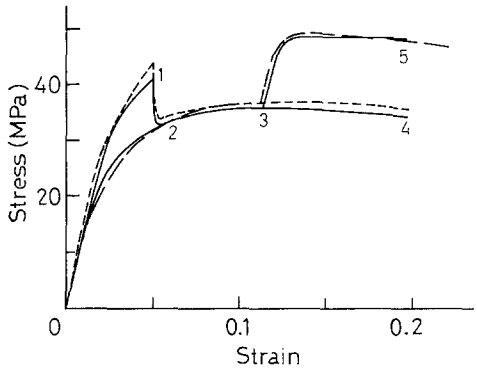

Figure 8 Experimental (– – –) and computed (——) stress–strain curves at sudden change of strain rate at 25° C. 1–2–3–4; $9 \times 10^{-3}\,\mathrm{sec}^{-1} \rightarrow 9 \times 10^{-5}\,\mathrm{sec}^{-1}$ and 1–2–3–5; $9 \times 10^{-5}\,\mathrm{sec}^{-1} \rightarrow 9 \times 10^{-3}\,\mathrm{sec}^{-1}$.

approaches the one obtained for a simple test conducted at the same strain rate.

Fig. 8 shows the effect of the sudden change in strain rate on the stress–strain curve. The specimen was compressed at a certain nominal strain rate to a predetermined strain and then the strain rate was suddenly changed to the other one 100 times higher or lower than the previous one. In the neighbourhood of the change point, the curve seems to have an elastic response and in excess of its neighbourhood, it gradually approaches and soon coincides with the curve obtained at the later strain rate from the beginning of the test. The solid lines are computational as discussed in the later section.

The experimental stress–strain curves at a combination test of constant deformation rate, stress relaxation, creep and constant deformation rate are shown in Fig. 9 where the solid curves are computational.

4. Constitutive model and discussion

Although much effort has been made to introduce a non-linearity into a constitutive law of visco-elastic solid, non-linear behaviours at finite strains have not been successfully understood. In the present paper, we consider the three-element solid model as a starting equation.

$$k\dot{\sigma} + \sigma = m\dot{\varepsilon} + g[\varepsilon] \qquad (1)$$

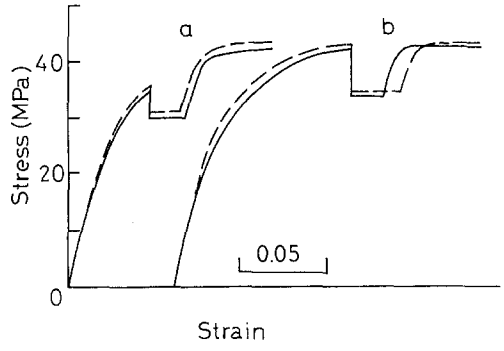

Figure 9 Experimental (– – –) and computed (——) stress–strain curves with complex strain histories at 25° C. a; constant nominal strain rate ($9 \times 10^{-4}\,\mathrm{sec}^{-1}$) (;c.n.s.r.) → 30 sec stress relaxation → 20 min creep → c.n.s.r. b; c.n.s.r. → 60 stress relaxation → 10 min creep → c.n.s.r.

or

$$\dot{\varepsilon} = (k/m)\dot{\sigma} + (\sigma - g[\varepsilon])/m \qquad (2)$$

where σ and ε are stress and strain, k and m are material constants, $g[\varepsilon]$, which is a linear function of ε, is an equiribrium stress–strain curve at a strain rate of $\dot{\varepsilon} = 0$ and the dot denotes the differentiation with respect to time. If the viscous resistance of the dashpot part in the three-elements model is replaced by an Eyring type equation in place of a Newton one, Equation 2 may be rewritten by

$$\dot{\varepsilon} = \dot{\sigma}/E + b \sinh \{c(\sigma - g[\varepsilon])\} \qquad (3)$$

where E is the instantaneous elastic modulus and b and c are constants. Equation 3 adopts a non-linearity in a negative manner. In order to introduce a non-linearity in the Equation 1 or 2 actively, k and m are assumed to be given by

$$k = k[\sigma - g[\varepsilon], \sigma, \varepsilon, \dot{\sigma}, \dot{\varepsilon}] \qquad (4)$$

$$m = kE \qquad (5)$$

and furthermore, $g[\varepsilon]$ is assumed to be a non-linear function of ε. The bracket $[\cdot]$ means the function of the argument. $\sigma - g[\varepsilon]$, the deviation of the current stress from the equiribrium stress, is called an over stress. This concept has been successfully applied to the stress–strain relations of metals. As the deformation progresses the micro-structure of the material will change and its anisotropy will develop. The present paper does not consider this aspect in a positive manner.

The k function can be determined by means of the stress relaxation tests through the equation

$$k = -(\sigma - g[\varepsilon])/\dot{\sigma} \qquad (6)$$

σ and $g[\varepsilon]$ being obtained on the relaxation records. Here the stress value obtained after an elapse of 24 h in the relaxation test was used as the equiribrium stress corresponding to the test strain (see the circles in Fig. 3). After an elapse of 24 h in the relaxation test, the ratio of the rate of stress decrease to the instantaneous modulus was of order of less than $10^{-12}\,\mathrm{sec}^{-1}$ which may be very small and therefore the stress reached at that time may reasonably be estimated to be the equiribrium stress. It may be desirable to concisely infer its experimental values through the relaxation tests for a short time interval. Here, we tried to estimate them from the 3 h relaxation tests. The σ (stress) against log time (t) curve during the relaxation period from 1 min to 3 h became linear. In the linear approximation of this curve by means of the least square method, the σ value at $t = 15$ h was confirmed to be nearly equal to the experimental one at $t = 24$ h. The experimental data marked by the circles at 15 and 45° C in Fig. 13 were obtained in this way. These values are not independent of the strain rate preceding the relaxation tests.

The values of k calculated in this way are plotted as a function of over stress for different temperatures in Fig. 10. $k[\cdot]$ is found to be a decreasing function of over stress and strain and is well described by

$$k = k_0 \exp\{-k_1[\varepsilon](\sigma - g[\varepsilon])\} \qquad (7)$$

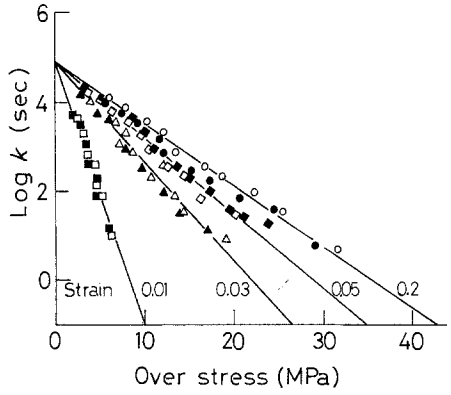

Figure 10 k in Equation 1 plotted against over stress diagram at different strains. the open and the solid marks correspond to the strain rates of $9 \times 10^{-4}\,\mathrm{sec}^{-1}$ and $9 \times 10^{-3}\,\mathrm{sec}^{-1}$ preceding the relaxation test.

where k_0 may be a material constant independent of temperature. Furthermore, $k_1[\varepsilon]$ can be approximated by

$$k_1[\varepsilon] = p_0 + p_1/(\varepsilon + p_2) \tag{8}$$

where p_0, and p_1 and p_2 are temperature dependent parameters. A comparison of Equation 8 with the experimental data at different temperatures is made in Fig. 11. Here the constant $p_2 = 0.000\,05$ is assumed to be temperature independent.

It is desirable to describe one more function $g[\varepsilon]$ in a suitable function of ε. The equiribrium curve expressing a slight work softening behaviour in PP can be well approximated by

$$\begin{aligned} g[\varepsilon] &= (g_m/f)\{\tanh(b\varepsilon/\varepsilon_m) - (\operatorname{sech} b_0)^2(b\varepsilon/\varepsilon_m)\} \\ f &= b_0(\tanh b_0)^2 + \tanh b_0 - b_0 \\ b &= b_1 + b_2 - b_2 \exp(-b_3\varepsilon) \\ b_1 &= f\varepsilon_m E/\{(\tanh b_0)^2 g_m\}, \quad b_2 = 2b_0 - b_1 \end{aligned} \tag{9}$$

where g_m is the maximum stress at the curve, b_0, b_3 and ε_m are temperature-independent parameters chosen so that the equation may agree with the experimental data. This approximation assumes that the initial tangential slope near $\varepsilon = 0$ is equal to the instantaneous modulus E.

The values of the constants in Equation 8 and 9 are plotted as a function of temperature in Fig. 12. The other constants of $p_2 = 5 \times 10^{-5}$, $b_0 = 2$, $b_3 = 80$ and $\varepsilon_m = 0.15$ are assumed to be temperature independent. Equation 9 with the constants chosen for every temperature, which is drawn by the solid curves marked g_1, g_2 and g_3 in Figs 3 and 13, is found to be in good agreement with the experimental equilibrium stresses. The static yield stress g_m, and the instantaneous elastic modulus E and the constants p_0 and p_1 can be approximated as a linear function of temperature by

$$\begin{aligned} g_m &= -0.294\,T + 106.3 \\ E &= -19.6\,T + 7122 \\ p_0 &= 3.39 \times 10^{-3}\,T - 0.774 \\ p_1 &= 1.36 \times 10^{-4}\,T - 0.0298 \end{aligned} \tag{10}$$

in the units of MPa and K where T is the absolute temperature.

By the above procedure, the non-linear constitutive Equation 1 is characterized and its predictive capability is able to be compared with the experimental data under various strain histories. However, in the case where the current strain will be below the previous one, these equations should be modified so that they can explain the effect of the strain histories given in the past. In this paper, the uni-

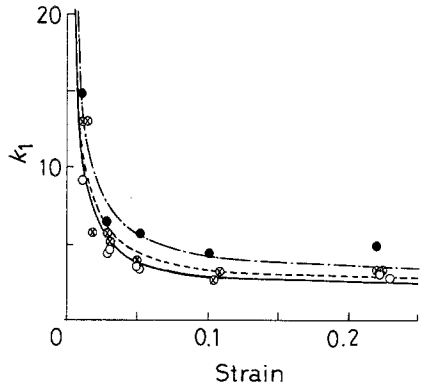

Figure 11 k_1 in Equation 1 as a function of applied strain at different temperatures (●; 45° C, ⊗; 25° C and ○; 15° C). The solid curves show Equation 8.

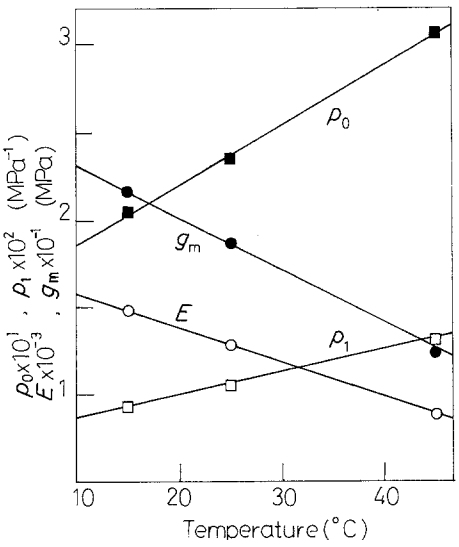

Figure 12 Temperature dependence of the constants included in Equations 8 and 9.

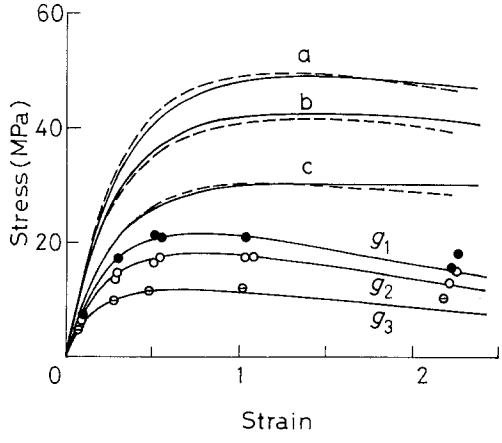

Figure 13 Comparison between experimental (– – –) and computed (——) stress–strain curves at the nominal strain rate of $9 \times 10^{-4}\,\mathrm{sec}^{-1}$ in different temperatures. The equiribrium stress–strain curves g_1, g_2 and g_3 are drawn based on Equation 9.

axial stress–strain curves without strain reversal are described.

Equation 1 with Equation 4 and 5 based on the over-stress concept is proved to explain some experimental facts in metals that (1) in a constant strain rate test, the stress–strain curve is equidistant to the equiribrium curve in the high strain range, (2) in the stress relaxation tests executed in the high strain region, the amount of stress drop for a given time interval is nearly independent of the strain, (3) in a creep test under a relatively high stress, three stages, i.e., primary, secondary and tertiary creep, is observable if the equiribrium curve depicts a work softening as shown in the present material PP, and so on. For proof of these matters see reference [5].

These predictions seem to be in good agreement with the present experimental results shown in Figs 3–6. The results computed from Equation 1 with the numerical constants given in the previous section are drawn by the solid curves and are compared with the experimental ones in Figs 3–9. It is found that Equation 1 based on the over stress theory well describes some interesting features on the stress–strain response in PP. This may show that Equation 1 becomes a powerful means in inferring the stress–strain behaviours with more complex strain histories.

In order to construct a non-linear constitutive model in polymers, the pressure dependent natures and furthermore the stress responses with strain reversal should be investigated in future.

References

1. K. C. VALANIS, *Arch. Mech.* **23** (1971) 517.
2. *Idem., ibid.* **23** (1971) 535.
3. L. E. MALVERN, *Trans. ASME, J. Appl. Mech.* **18** (1951) 269.
4. E. KREMPL, *Trans. ASME, J. Engng Mater. Tech.* **101** (1979) 380.
5. M. C. LIU and E. KREMPL, *J. Mech. Phys. Solids* **27** (1979) 377.
6. M. KITAGAWA, Y. SAKAI and M. KAWAGOE, *J. Mater. Sci.* **15** (1980) 1463.

Received 8 December 1987
and accepted 29 April 1988